JVSTB
JOURNAL OF VACUUM SCIENCE AND TECHNOLOGY B

Study of the interaction of polymethylmethacrylate fragments with methyl isobutyl ketone and isopropyl alcohol

Mohammad Ali Mohammad, Kolattukudy Poulose Santo, Steven K. Dew, and Maria Stepanova

Citation: J. Vac. Sci. Technol. B **30**, 06FF11 (2012); doi: 10.1116/1.4766318
View online: http://dx.doi.org/10.1116/1.4766318
View Table of Contents: http://avspublications.org/resource/1/JVTBD9/v30/i6
Published by the AVS: Science & Technology of Materials, Interfaces, and Processing

Related Articles

Ultraviolet curable branched siloxanes as low-k dielectrics for imprint lithography
J. Vac. Sci. Technol. B 31, 011601 (2013)

Fundamental study of extreme UV resist line edge roughness: Characterization, experiment, and modeling
J. Vac. Sci. Technol. B 30, 06F506 (2012)

Large area nanofabrication of butterfly wing's three dimensional ultrastructures
J. Vac. Sci. Technol. B 30, 061802 (2012)

Release layer-free acrylate resins with segregation auxiliary agents for ultraviolet nanoimprinting
J. Vac. Sci. Technol. B 30, 06FB05 (2012)

Gas Phase Deposition of Trichloro(1H,1H,2H,2H-perfluorooctyl)silane on Silicon Dioxide, by XPS
Surf. Sci. Spectra 17, 87 (2010)

Additional information on J. Vac. Sci. Technol. B

Journal Homepage: http://avspublications.org/jvstb
Journal Information: http://avspublications.org/jvstb/about/about_the_journal
Top downloads: http://avspublications.org/jvstb/top_20_most_downloaded
Information for Authors: http://avspublications.org/jvstb/authors/information_for_contributors

ADVERTISEMENT

Study of the interaction of polymethylmethacrylate fragments with methyl isobutyl ketone and isopropyl alcohol

Mohammad Ali Mohammad[a)]
Department of Electrical and Computer Engineering, University of Alberta, Edmonton, Alberta T6G 2V4, Canada

Kolattukudy Poulose Santo
Department of Electrical and Computer Engineering, University of Alberta, Edmonton, Alberta T6G 2V4, Canada and National Institute for Nanotechnology NRC, 11421 Saskatchewan Drive, Edmonton, Alberta T6G 2M9, Canada

Steven K. Dew
Department of Electrical and Computer Engineering, University of Alberta, Edmonton, Alberta T6G 2V4, Canada

Maria Stepanova[b)]
Department of Electrical and Computer Engineering, University of Alberta, Edmonton, Alberta T6G 2V4, Canada and National Institute for Nanotechnology NRC, 11421 Saskatchewan Drive, Edmonton, Alberta T6G 2M9, Canada

(Received 17 July 2012; accepted 22 October 2012; published 9 November 2012)

Exposure of polymethylmethacrylate (PMMA) during electron beam lithography (EBL) produces small polymer fragments that dissolve rapidly during the development process. The resist dissolution behavior varies greatly depending on the nature of the developer (solvent) and therefore influences the selection of the EBL parameters, such as dose (sensitivity). A molecular scale examination of the development process is necessary to elucidate the resist–developer interaction mechanisms. In this work, the authors investigate the interaction of short PMMA chains (containing up to 10 MMA units) with common developer components methyl isobutyl ketone (MIBK) and isopropyl alcohol (IPA). For this purpose, the authors conduct molecular dynamics simulations using the Accelrys Materials Studio package. The simulation results were used to characterize the mixtures in the spirit of the Flory–Huggins theory of polymers and also to extract the diffusivities. The authors found that the behavior of PMMA fragments differed considerably in MIBK as compared with IPA. PMMA fragments containing more than three monomers exhibit stronger attractive interaction with MIBK. For all fragment sizes simulated, the diffusivity of PMMA fragments is 60–160% higher in MIBK as well. Similarly, the authors observed differences in the gyration radii. The authors conclude that the kinetic factor seems to be more significant as compared to affinity factor when accounting for differences in exposure sensitivities due to developer selection. © *2012 American Vacuum Society*. [http://dx.doi.org/10.1116/1.4766318]

I. INTRODUCTION

Polymethylmethacrylate (PMMA) is the most widely used resist for electron beam lithography (EBL). PMMA formulations for nanofabrication contain chains that are thousands of monomer units in length. PMMA has been traditionally and predominantly used as a positive-tone resist; however, it may also be used as a negative-tone resist if an approximately one-order higher exposure dose is used. Under electron beam irradiation, the various physicochemical changes giving rise to positive and negative-tone behavior occur simultaneously[1] with the dominant mechanism dependent on various material and experimental factors. Although negative-tone PMMA behavior may yield processing advances under special processing conditions,[2] this regime is rarely used for actual nanofabrication.

In positive-tone regimes the chain scission prevails, which drastically reduces the chain lengths. Depending on the dose, PMMA may degrade down to single monomer[3,4] units; however, due to the statistical nature of electron scattering a typical electron beam exposed volume will contain a distribution of chain lengths.[5] Other proposed electron beam exposure products of PMMA include gaseous and liquid volatiles such as CO_2, CH_4, CH_3OH, etc., and occasionally, derivatives with one unsaturated bond; however, such unsaturated specie has a very low production efficiency. Due to the above reasons, at nominal clearance doses, it is safe to assume that the scission products of PMMA are shorter versions of the original unexposed chains. In a suitable developer[6] (solvent), it has been assessed that small PMMA chains less than approximately 10 monomers in length[5] are preferentially soluble, with the details depending on the developer.

It is known that the development process depends on the kinetic and thermodynamic compatibility of the resist and the developer.[7] A number of developers have been employed

a)Electronic mail: mam20@ualberta.ca
b)Electronic mail: maria.stepanova@nrc-cnrc.gc.ca

for PMMA, e.g., methyl isobutyl ketone (MIBK), isopropyl alcohol (IPA), ethoxyethanol (Cellosolve), xylene, GG-developer (LIGA developer), etc., and it has been observed that the sensitivity (electron dose required) for EBL patterning varies depending on the strength of the developer. For example IPA, a weak developer for PMMA,[8] requires up to 4.3 times higher dose for EBL as compared to MIBK, which is a strong developer for PMMA. From a processing perspective, often a mixture of strong and weak developers is desired, e.g., MIBK:IPA in various volume fractions.[9] Such a binary component developer yields significant improvements in feature resolution at a cost of process sensitivity. Understanding the differences in sensitivity with changing developer requires an examination of the postexposure development stage at the molecular scale. Such understanding is crucial for rational optimization of the EBL process as the wet development stage is the most limiting step in nanolithography.

The solvent penetration into the polymer and subsequent polymer dissolution is kinetically controlled.[10] The diffusivity of the solute can be described by an Arrhenius rate law, $D = D_0 e^{-\frac{E_a}{kT}}$, where E_a is the activation energy, k is the Boltzmann's constant, T is the temperature, and D_0 is the coefficient. This coefficient is a function of fragment molecular weight M_f and solvent characteristics. The mobility of polymer fragments decreases with increasing fragment size.[4] Various functional forms for D_0 exist in literature, for example, $D_0 \sim M_f^{-\alpha}$ where α is a fragment size dependent exponent. The value of α varies from ≤ 1 in a dilute solution[11] or in a polymer melt containing only small fragments (Rouse regime) to ~ 2 in dense polymer melts (entanglement regime).[12–14] The fragment molecular weight (chain length n) in turn can be related to electron beam exposure dose.[12,15]

The affinity of resist–developer mixture can be studied using the Flory–Huggins (F–H) lattice theory.[16,17] In contrast with regular solution theory,[18] the F–H theory successfully handles the mixing of species with very different molecular weights, such as a polymer and a developer liquid. Predicting the miscibility of such a binary mixture requires computation of the F–H interaction parameter (χ). A number of researchers from the EBL community such as Sharma *et al.*[19] and Hasko *et al.*[20] have qualitatively discussed the development stage using arguments from the F–H theory. Hang *et al.*[21] have calculated the χ parameters using the Hansen solubility parameters (SP) method for identifying PMMA removers. Similarly, Olynick *et al.*[22] have used Hansen's SP for calculating χ for mixtures of calixarene resist and numerous liquids, and have found a correlation between resist–developer solubility and contrast (γ). None of these studies take into consideration dissolution of exposed fragments, and instead rely on tabulated data of the Hansen's SP for calculations. Moreover, the approach for calculating χ based on Hansen SP suffers from certain drawbacks, e.g., it is unable to describe the concentration dependence of χ,[23] yields only positive χ values,[17,23] and has a limited applicability for hydrogen bonds or other strong polar interactions.[17]

Experimental studies of the dissolution of low molecular weight resist fragments are challenging due to their small size and low concentration in solution. Sizes of PMMA fragments which typically arise in EBL processes are less than 5 nm and have concentrations in the ng/ml to μg/ml range under typical experimental conditions. Molecular dynamics (MD) simulation is a suitable technique that can be used to meet this challenge. The nanolithography community is increasingly using MD for various applications. MD has been used for studying the acid diffusion in chemically amplified resists,[24] the effects of scribing feed in scanning probe lithography,[25] and more recently for studying the various aspects of nanoimprint lithography.[26–28] MD has also been used extensively to study polymer behavior in various environments; in regard to polymer miscibility, Apel *et al.*[29] have studied the dissolution of unexposed PMMA chains (degree of polymerization $n \geq 1000$) in benzene. However, such lengths are not representative of typical exposed PMMA fragments and exhibit different dissolution trends. Patnaik and Pachter[30] have studied the miscibility of PMMA chains ($n \sim 1$, 2, 3, 100, 200) in a low molecular mass liquid crystal and calculated the interaction parameter χ based on MD simulations using BLENDS and DISCOVER software modules (Accelrys Materials Studio Package[31]). De Arenaza *et al.*[32] and Fu *et al.*[33] have also used Accelrys Materials Studio for calculating the χ parameter for various polymer blends. In addition to allowing researchers to address the interaction of various species, MD has the advantage to enable the study of kinetic and statistical-mechanical aspects.

In this work, we study the miscibility of short PMMA chains ($n \leq 10$) with MIBK and IPA developers by conducting MD simulations in Accelrys Materials Studio. Although the resist–developer interface is not included in these simulations explicitly, the simulation setup is chosen such that both solute–solute and solute–solvent interactions occurring in a proximity of the resist–developer interface could be addressed. The simulation data are characterized using the F–H theory, and the fragment–developer interaction parameters are computed. The differences in the radii of gyration in MIBK and IPA are examined, and the fragment diffusion coefficients (diffusivities) are also extracted. The behavior of PMMA fragments in both developers is compared in light of lithography observations.

II. MODELING AND ANALYSIS

We study the miscibility of PMMA fragments with degree of polymerization $n = 1$, 2, 3, 4, 6, 8, and 10 in developers MIBK and IPA (see Fig. 1). Prior to running simulations for the binary mixtures PMMA(n):MIBK and PMMA(n):IPA, we perform MD simulations for each of the pure components PMMA(n), MIBK, and IPA. Where the physical properties of pure components are experimentally known, e.g., the densities of MIBK and IPA, these known values are used to find the optimal simulation parameters and to compute the simulation system properties, such as the volume and potential energy. Where the properties are experimentally unknown, e.g., in the case of PMMA(n) for all n, these properties can be computed with confidence using the optimized MD simulation parameters obtained

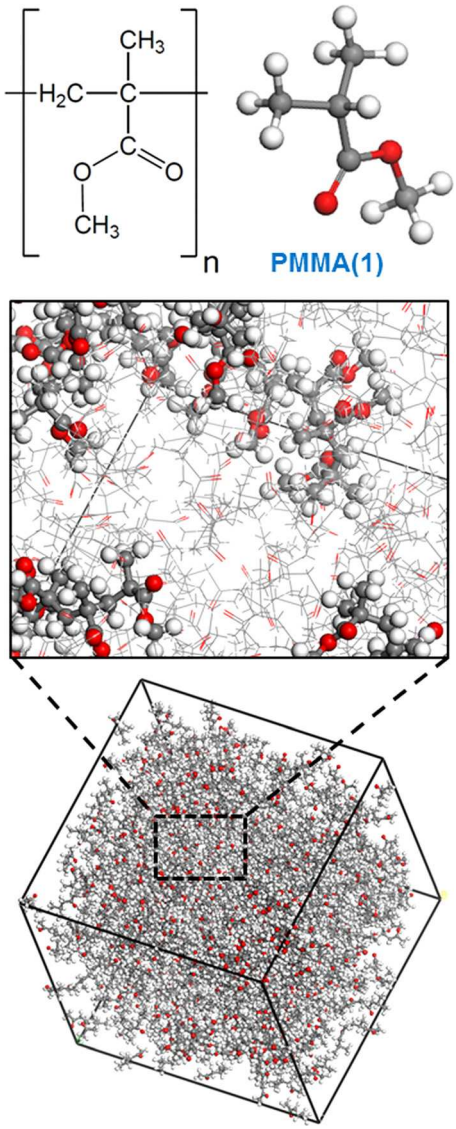

FIG. 1. (Color online) Visualization of a PMMA monomer PMMA(1) with its chemical formula and an MD simulation box containing PMMA(10) chains in MIBK developer.

previously. The obtained quantities from the pure components are used as input data for simulating the mixtures PMMA(n):MIBK and PMMA(n):IPA.

A. Molecular dynamics simulations

The simulation strategy is summarized in Fig. 2. For each component (PMMA(n), MIBK, and IPA), a set of molecules is assembled and energy minimized. An isothermal–isobaric (NPT) ensemble dynamics simulation is conducted to determine the system density. The equilibrated system is subjected to a canonical (NVT) ensemble dynamics simulation to obtain the potential energies. The above process is repeated for the PMMA(n):MIBK and PMMA(n):IPA binary mixtures following which the F–H interaction parameters can be calculated. The binary mixtures are also subjected to a microcanonical (NVE) ensemble dynamics simulation—the result of which is analyzed to obtain the fragment diffusivities and radii of gyration.

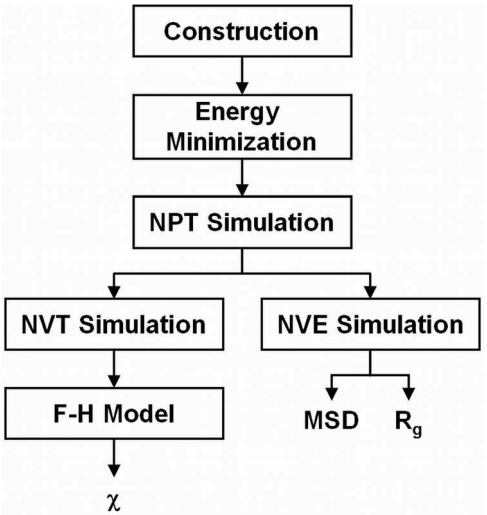

FIG. 2. Flowchart of MD simulation strategy.

All of the MD simulations and analysis, except for the calculation of the F–H interaction parameters, are conducted using Accelrys Materials Studio[31] package. All simulation systems are constructed at ambient conditions (295 K and 1 atm) with periodic boundary conditions using the AMORPHOUS CELL module. The default force-field used by Materials Studio is COMPASS,[34] which is suitable for our systems. The AMORPHOUS CELL module is also used for the energy minimization (10 000–100 000 steps) using the conjugate gradient method. The DISCOVER module is used for all NPT, NVT, and NVE dynamics runs. The system energies, fragment mean squared displacement (MSD), and gyration radii are obtained using the FORCITE module. Where applicable, the Andersen[35] thermostat (collision ratio 1) was used for the temperature control and the Berendsen[36] barostat (decay factor 0.08–0.09 ps) was used for the pressure control. Group-based summations were used for the nonbond (van der Waals and Coulomb) interactions and a cutoff of 12.5 Å (3 Å spline, 1 Å buffer, long range correction) was used.[34] The charge groups were assigned manually for the developers and automatically for the PMMA fragments. The effect of hydrogen bonding is implicitly contained in the nonbond interaction terms. Constraint algorithms were not used. These simulation parameters were determined through extensive testing and verification, e.g., the Andersen[35] thermostat and Berendsen[36] barostat were found to be the most accurate in maintaining the temperature and pressure within desired limits. Similarly, the simulation times for individual dynamics runs were carefully selected. Unless stated, the parameters are kept constant in all simulations.

1. Developer simulations

The experimental densities of developers MIBK and IPA are known to be 0.801 and 0.785 g/cm^3, respectively. Two separate systems containing 500 molecules each of MIBK (9500 atoms) and IPA (6000 atoms) were constructed, energy minimized, and subjected to NPT dynamics for

1000 ps (1 fs step sizes) using the previously described parameters. The simulated densities were found to be 0.805 and 0.803 g/cm^3, respectively, within 2.3% of experimentally known values.[37] The density equilibrated systems were further subjected to NVT dynamics for 1000 ps (1 fs steps) to determine the potential energies.[37]

2. PMMA fragment simulations

The first step is to obtain the unknown densities of PMMA fragments by NPT dynamics. In this work, we consider only the isotactic conformations of PMMA fragments. The number of PMMA(n) molecules used for each fragment size is given in Table I. We attempted to keep the number of residues (monomers in system) constant; however, more important was maintaining the minimum image convention, i.e., the unit cell's length is at least the length of the PMMA(n) molecule at full stretch + (2 × cutoff radius) + 5 Å. Therefore, each unit cell has 9000–10 000 atoms for PMMA(1)–PMMA(6) and approximately 18 000 atoms for larger chain sizes corresponding to unit cell sizes of 45.5–57.4 Å. The total NPT simulation duration was 1250 ps (1 fs steps) which comprised a 1000 ps equilibration run and a 250 ps production run. Following NPT dynamics, the PMMA(n) systems were subjected to NVT dynamics for 1000 ps (at 1 fs steps) to obtain the potential energies.[37]

3. PMMA fragment and developer mixture simulations

The PMMA fragment and developer mixture systems are constructed such that the polymer fraction is approximately 16.7% by mass. Therefore, this polymer solution may be considered as semidilute and such a polymer concentration is appropriate for studying the resist–developer interface environment. The number of molecules in the PMMA(n):MIBK and PMMA(n):IPA binary mixtures is given in Table I. In both mixtures, the number of PMMA(n) residues is kept constant while simultaneously maintaining the minimum unit cell size as described in Sec. II A 2. The unit cell sizes for the PMMA(n):MIBK and PMMA(n):IPA mixtures range from 52.2 to 52.8 Å and from 52.5 to 53.0 Å, corresponding to 13 324–13 440 and 13 824–14 040 atoms, respectively.[37] The binary systems were subjected to NPT dynamics for 350 ps (0.5 fs step size for improved accuracy) including a 250 ps equilibration and a 100 ps production run followed by NVT dynamics for 1000 ps (at 1 fs steps).

TABLE I. MD simulation composition for PMMA fragments and mixtures.

n	PMMA(n) molecules	PMMA(n): MIBK molecules	PMMA(n): IPA molecules
1	600	120:600	120:1000
2	300	60:600	60:1000
3	200	40:600	40:1000
4	150	30:600	30:1000
6	100	20:600	20:1000
8	150	15:600	15:1000
10	120	12:600	12:1000

Number of atoms in PMMA pure component simulations 9200–18 340, in PMMA(n):MIBK mixtures 13 224–13 440, and in PMMA(n):IPA mixtures 13 824–14 040.

B. Analysis of short chain miscibility

The Flory–Huggins equation for the free energy of mixing[17] consists of both entropic and enthalpic parts. As the entropy contribution generally favors mixing, the determining factor for miscibility in the F–H equation is the enthalpic part, which reads

$$\chi = \frac{\Delta H}{RT\varphi_s\varphi_p}, \tag{1}$$

where ΔH is the change in the enthalpy of mixing; R is the gas constant; T is the temperature; and φ_s and φ_p, respectively, are the solvent and polymer volume fractions. In Eq. (1), ΔH is related to the change in the energy of mixing ΔE_{mix} by a simple relation $\Delta H = \Delta E_{mix}/N_{latt}$, where N_{latt} is the number of so-called lattice sites in the system. Further, $\Delta E_{mix} = E_{mix} - n_s E_{ss} - n_p E_{pp}$, where E_{mix} is the energy of the binary mixture and E_{ss} and E_{pp} are the energies of developer and PMMA(n) fragments taken separately, and n_s and n_p are the number of developer and PMMA(n) fragments, respectively. Therefore, we can rewrite Eq. (1) in terms of quantities that can be obtained through MD simulations as follows:

$$\chi = \frac{E_{mix} - n_s E_{ss} - n_p E_{pp}}{RTN_{latt}\varphi_s\varphi_p}. \tag{2}$$

The aforementioned approach has been implemented in MATLAB and is referred to as the F–H model in Fig. 2. It is known that for a given polymer–solvent mixture, the components are miscible under the condition $\chi < \chi_c$ where χ_c is the critical interaction parameter,[17] given by

$$\chi_c = \frac{1}{2}\left(1 + \frac{1}{\sqrt{n}}\right)^2. \tag{3}$$

From this equation, we observe that $\chi_c = 2$ for $n = 1$, and $\chi_c \to 0.5$ as $n \to \infty$. Therefore, in a binary mixture, phase separation or segregation of components occurs for large chain polymers as long as χ is larger than $\chi_c = 0.5$ with χ_c increasing as the polymer chain size decreases.

C. Analysis of short chain diffusivity and gyration radius

In an NVE dynamics run, the thermostat and barostat are turned off and a trajectory file containing sequential snapshots of fragment motions through the developer can be obtained. After selecting the fragments of interest, the MSD can be obtained using the FORCITE module. Excluding the initial few snapshots where the fragments exhibit ballistic motion, the MSD plot would normally be linear. Calculating the slope of the linear region yields the fragment diffusivity D,

$$D = \frac{1}{6N}\lim_{t\to\infty}\frac{d}{dt}\sum_{i=1}^{N}\langle[r_i(t) - r_i(0)]^2\rangle, \tag{4}$$

where N is the number of atoms in the system, and r_i is the position of the ith atom at a time snapshot (simulation frame) t. Calculating the diffusivity of each fragment and plotting the diffusivity versus the fragment size allow extraction of the exponent α which determines the fragment size dependence of the diffusivity, $D_0 \sim M_f^{-\alpha}$. The radius of gyration R_g can also be found for the fragments of interest using the FORCITE module after an NVE simulation.

III. RESULTS AND DISCUSSION

The NPT and NVT dynamics simulations were conducted sequentially for all pure components (PMMA(n), MIBK, and IPA) and binary mixtures (PMMA(n):MIBK and PMMA(n):IPA). Results from all simulations are archived in Ref. 37. In this section, we present the relevant results from the binary mixture simulations. The equilibrated volumes and densities of the PMMA(n):MIBK and PMMA(n):IPA binary mixtures after NPT dynamics are presented in Fig. 3. As the PMMA fragments become larger, the volume and density rapidly change and subsequently tend to saturate. The increase in mixture density with increasing PMMA fragment size is consistent with the PMMA(n) NPT simulations.[37] As the PMMA fragments become larger, the density of the system should approach the PMMA bulk density of 1.19 g/cm^3. The potential energies of the binary mixtures after NVT dynamics are presented in Fig. 4. The large negative energies of the mixture suggest an exothermic (spontaneous) mixing process, consistent with our expectations. The difference in the energies of mixing of PMMA fragments with MIBK and IPA is not directly representative of the relative affinities because of different masses and volumes of the solvents involved. These factors are accounted for in the Flory–Huggins mixing parameter χ, which we have computed in order to compare the affinities.

The Flory–Huggins χ parameters for the binary mixtures are presented in Fig. 5. With increasing PMMA fragment sizes, initially the χ parameters rapidly decrease followed by a saturation behavior. With the exception of PMMA monomers ($n=1$) and dimers ($n=2$) in MIBK, all small PMMA fragments exhibit a tendency to mix with MIBK and IPA developers. The behavior of PMMA monomers and dimers can be interpreted as limited miscibility with MIBK developer.

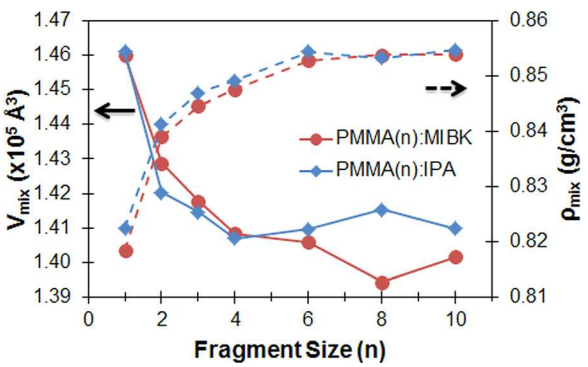

FIG. 3. (Color online) Volume and density of mixture for PMMA fragments containing n monomers in MIBK (circles) and IPA (diamonds) developers obtained after isothermal–isobaric (NPT) ensemble simulation.

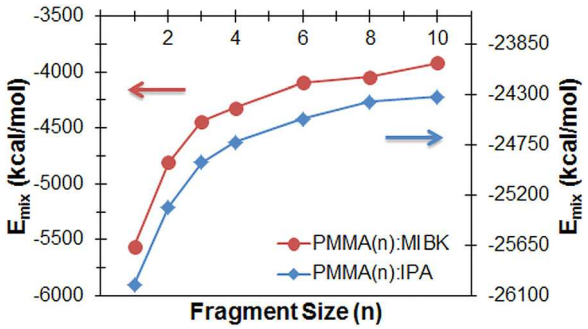

FIG. 4. (Color online) Energies of mixture for PMMA fragments containing n monomers in MIBK (circles) and IPA (diamonds) developers obtained after canonical (NVT) ensemble simulation.

Limited miscibility with a solvent developer may be interpreted as very small fragments tending to aggregate when exposed to the solvent. This hypothesis is currently under investigation. According to Fig. 5, χ decreases with increasing fragment size and tends to saturate beyond fragment sizes $n=6$. PMMA fragments with $n>3$ exhibit somewhat stronger attractive interaction with MIBK as compared to IPA. However, this trend does not fully explain the observed strong differences in sensitivities between the developers and their mixtures observed experimentally.[8]

Since the described simple considerations of intermolecular affinity appear to be insufficient to explain the different solubility of PMMA in two developers, the data provided by MD need to be studied in further detail to understand the dissolution behavior. Therefore, we have analyzed the radius of gyration (R_g) of PMMA fragments of various sizes, as provided by the NVE simulations. The corresponding distributions of R_g for $n=1$ and 10 in MIBK and IPA solvents are presented in Fig. 6. For the monomer [Fig. 6(a)], there is no difference in R_g between the two developers, as one could expect; however, in the case of PMMA(10) [Fig. 6(b)] the fragments exhibit a different R_g distribution in IPA as compared to MIBK. As can be seem from Fig. 6(b), PMMA(10) fragments exposed to IPA exhibit four distinct maxima in the R_g distribution at 5.5, 6.2, 6.7, and 7.3 Å. The most probable gyration radius in IPA (6.2 Å) is smaller than in MIBK (6.5 Å).

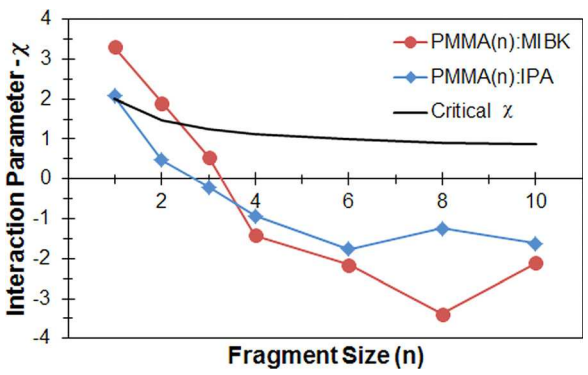

FIG. 5. (Color online) Flory–Huggins interaction parameters for PMMA fragments containing n monomers in MIBK (circles) and IPA (diamonds) developers. Also plotted is the critical interaction parameter below which mixing is promoted.

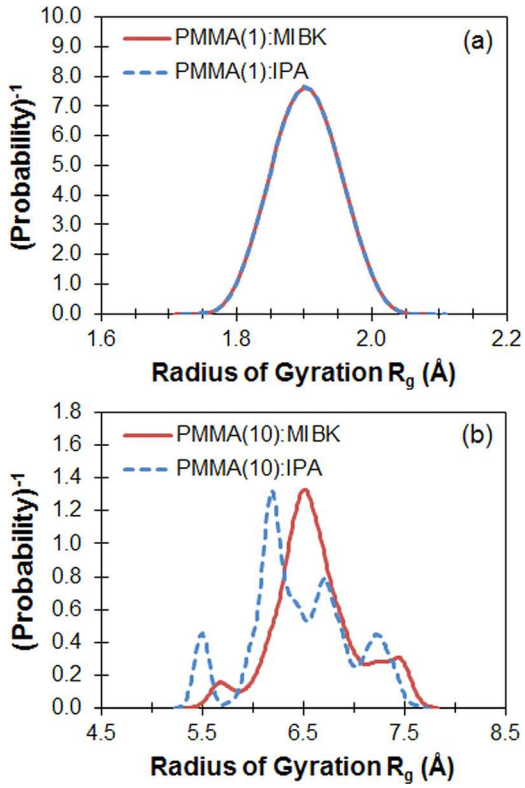

FIG. 6. (Color online) Radii of gyration of PMMA fragments containing (a) one monomer and (b) ten monomers in MIBK (solid lines) and IPA (dashed lines) developers obtained after microcanonical (NVE) ensemble simulation.

The results shown in Fig. 6 are compatible with the known dependence of the polymer chain conformation on the solvent quality. Generally, polymers exhibit expanded conformations in good solvents whereas they adopt collapsed (folded) conformations as well as tend to aggregate in poor solvents. Thus, a fragment with an expanded conformation will have a large R_g, whereas a fragment with a folded conformation will have a smaller R_g. This property has been employed by Yasin *et al.*[38] to select the proper PMMA developer mixture for achieving ultrasmall (<5 nm) nanolithography patterns using ultrasonic development. Further to this, Nakamura *et al.*[39,40] and Nakata *et al.*[41] have performed experimental studies of dissolution of long PMMA chains ($n \sim 16\,000$) in an alcohol and water mixture and found that both chain aggregation and chain collapse occur in such mixtures.[39] They also demonstrated that chain collapse tends to occur before the aggregation.[41]

Therefore, our simulation results from Fig. 6(b) can be interpreted as the PMMA fragments tending to adopt relatively collapsed conformations, represented by the peaks of R_g at 5.5 and 6.2 Å when exposed to IPA, a weaker solvent than MIBK. Although it is unclear yet from the MD data whether chain aggregation also is occurring in IPA solvent, one can conclude that the conformations adopted by longer chains in IPA are different from those in MIBK. This may explain why the interaction parameters χ of longer PMMA fragments in MIBK and IPA are close: after equilibration, the flexible chains adopt such a configuration that their affinity to either solvent is increased, leading to similar χ parameters. However, the experimentally observed differences in the performance of the MIBK and IPA solvents still require an explanation, for which reason we have also computed the diffusivities of PMMA fragments in the two solvents.

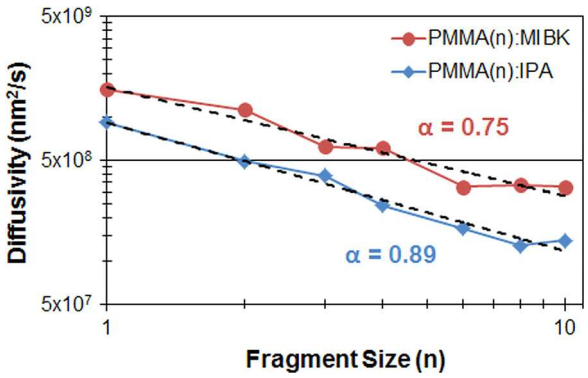

FIG. 7. (Color online) Diffusivity of PMMA fragments containing n monomers in MIBK (circles) and IPA (diamonds) developers computed from MSD obtained after microcanonical (NVE) ensemble simulation. The power law (const. $\times n^{-\alpha}$) fitting parameters (α) are also presented for both developers.

The diffusivity of PMMA fragments in MIBK and IPA is presented in Fig. 7. The decreasing diffusivity with increasing fragment lengths is evident as expected and the power law fitting parameter α is close to 1 in agreement with the Rouse regime.[14] The magnitude of PMMA fragment diffusivities (between 6×10^7 and 7×10^8 nm^2/s) in MIBK and IPA are also compatible with the experimentally measured coefficients of self-diffusion of various compounds such as hydrocarbons, which is on the order of 10^8 nm^2/s.[42] Finally, we observe that the diffusivity of PMMA fragments is 60–160% higher in MIBK as compared to IPA. Therefore, we conclude that the kinetic factor seems to be more significant as compared to thermodynamic factors when accounting for differences in EBL process sensitivities due to developer selection.

IV. CONCLUSIONS AND RECOMMENDATIONS

In order to understand the EBL development process, we have conducted a MD study of the dissolution of small PMMA chains containing up to 10 monomers in MIBK and IPA developers. Using Flory–Huggins theory of polymers, we calculate the fragment–developer interaction parameters. In addition to helping understand the dissolution behavior, calculation of the F–H χ parameter also allows the parameterization of statistical-mechanical and kinetic theories of resist dissolution[43] required for the rigorous modeling[44] of the development process. Furthermore, we extract the fragment diffusivities and examine the gyration radii in both developers. We observe that MD reveals differences in statistical-mechanical properties, miscibility, and kinetic behaviors of PMMA in MIBK and IPA solvents. In summary, we have the following conclusions:

(1) Larger PMMA fragments ($n > 3$) exhibit a slightly stronger attractive interaction with MIBK as compared to IPA.

(2) When exposed to IPA, PMMA fragments tend to adopt smaller gyration radii than in MIBK. Preferred gyration radii have been identified.
(3) The diffusivity of PMMA fragments is 60–160% higher in MIBK as compared to IPA.

We conclude that the difference in experimentally observed dissolution behavior of PMMA resist in the various developers can largely be attributed to the kinetic factor (difference in diffusivities). The hypothesized tendency of PMMA fragments to collapse and/or aggregate when exposed to IPA, as well as entropic factors, could also play a role. Recommendations for further work include (1) simulating larger model systems including longer chains and longer time durations, (2) addressing more solvents to include very strong solvents and nonsolvents such as acetone and water, respectively, (3) studying the dissolution behavior of PMMA fragments in mixed solvents such as MIBK + IPA and IPA + Water, etc., using modified Flory–Huggins equations, and (4) studying the PMMA fragment transport away from the resist surface using multiscale modeling techniques.

ACKNOWLEDGMENTS

The authors would like to thank Phillip Choi, Nikolay Blinov, Sarthak Patel, Taras Fito, Oliver Stueker, and Bilkiss Issack for helpful discussions. In addition, the financial support of NRC-NINT, NSERC, Alberta Innovates, Alberta Advanced Education and Technology (AAE&T), and iCORE is gratefully acknowledged.

[1]I. Brodie and J. J. Muray, *The Physics of Micro/Nano-Fabrication* (Springer, New York, 2010), p. 188.
[2]A. P. Adeyenuwo, M. Stepanova, and S. K. Dew, J. Vac. Sci. Technol. B **29**, 06F312 (2011).
[3]J. O. Choi, J. A. Moore, J. C. Corelli, J. P. Silverman, and H. Bakhru, J. Vac. Sci. Technol. B **6**, 2286 (1988).
[4]B. A. Miller-Chou and J. L. Koenig, Prog. Polym. Sci. **28**, 1223 (2003).
[5]M. Aktary, M. Stepanova, and S. K. Dew, J. Vac. Sci. Technol. B **24**, 768 (2006).
[6]A liquid or mixture of liquids whose miscibility discriminates based on the molecular weight of the solute is known as a developer solvent. A regular solvent (or remover or stripper in microfabrication jargon) is a liquid or mixture of liquids that dissolves the solute regardless of its molecular weight.
[7]J. S. Greeneich, J. Electrochem. Soc. **122**, 970 (1975).
[8]J.-S. Wi, H.-S. Lee, and K.-B. Kim, Electron. Mater. Lett. **3**, 1 (2007), available at http://www.e-eml.org/upload/04218154.pdf.
[9]MicroChem PMMA Data Sheet, retrieved September 22, 2012, http://www.microchem.com/pdf/PMMA_Data_Sheet.pdf.
[10]J. González-Benito and J. L. Koenig, Polymer **47**, 3065 (2006).
[11]L. Masaro and X. X. Zhu, Prog. Polym. Sci. **24**, 731 (1999).
[12]M. A. Mohammad, T. Fito, J. Chen, M. Aktary, M. Stepanova, and S. K. Dew, J. Vac. Sci. Technol. B **28**, L1 (2010).
[13]P. G. de Gennes, J. Chem. Phys. **55**, 572 (1971).
[14]V. A. Harmandaris, V. G. Mavrantzas, D. N. Theodorou, M. Kröger, J. Ramírez, H. C. Öttinger, and D. Vlassopoulos, Macromolecules **36**, 1376 (2003).
[15]M. A. Mohammad, T. Fito, J. Chen, S. Buswell, M. Aktary, M. Stepanova, and S. K. Dew, Microelectron. Eng. **87**, 1104 (2010).
[16]P. J. Flory, *Principles of Polymer Chemistry* (Cornell University Press, New York, 1953), p. 495.
[17]M. Rubinstein and R. H. Colby, *Polymer Physics* (Oxford University Press, New York, 2003), pp. 137–170.
[18]J. H. Hildebrand, Nature **168**, 868 (1951).
[19]V. K. Sharma, S. Affrossman, and R. A. Pethrick, Br. Polym. J. **16**, 73 (1984).
[20]D. G. Hasko, S. Yasin, and A. Mumtaz, J. Vac. Sci. Technol. B **18**, 3441 (2000).
[21]Q. Hang, D. A. Hill, and G. H. Bernstein, J. Vac. Sci. Technol. B **21**, 91 (2003).
[22]D. L. Olynick, P. D. Ashby, M. D. Lewis, T. Jen, H. Lu, J. A. Liddle, and W. Chao, J. Polym. Sci., Part B: Polym. Phys. **47**, 2091 (2009).
[23]S. Patel, A. Lavasanifar, and P. Choi, Biomacromolecules **9**, 3014 (2008).
[24]G. P. Patsis and N. Glezos, Microelectron. Eng. **46**, 359 (1999).
[25]T.-H. Fang, C.-I. Weng, and J.-G. Chang, Surf. Sci. **501**, 138 (2002).
[26]A. Taga, M. Yasuda, H. Kawata, and Y. Hirai, J. Vac. Sci. Technol. B **28**, C6M68 (2010).
[27]K. Tada, M. Yasuda, G. Tan, Y. Miyake, H. Kawata, M. Yoshimoto, and Y. Hirai, J. Vac. Sci. Technol. B **29**, 06FC11 (2011).
[28]M. Yasuda, K. Araki, A. Taga, A. Horiba, H. Kawata, and Y. Hirai, Microelectron. Eng. **88**, 2188 (2011).
[29]U. M. Apel, R. Hentschke, and J. Helfrich, Macromolecules **28**, 1778 (1995).
[30]S. S. Patnaik and R. Pachter, Polymer **43**, 415 (2002).
[31]Accelrys Materials Studio Software, San Diego, CA, USA, retrieved September 22, 2012, http://accelrys.com/products/materials-studio/.
[32]I. M. de Arenaza, E. Meaurio, B. Coto, and J.-R. Sarasua, Polymer **51**, 4431 (2010).
[33]Y. Fu, L. Liao, Y. Lan, L. Yang, L. Mei, Y. Liu, and S. Hu, J. Mol. Struct. **1012**, 113 (2012).
[34]H. Sun, J. Phys. Chem. B **102**, 7338 (1998).
[35]H. C. Andersen, J. Chem. Phys. **72**, 2384 (1980).
[36]H. J. C. Berendsen, J. P. M. Postma, W. F. van Gunsteren, A. DiNola, and J. R. Haak, J. Chem. Phys. **81**, 3684 (1984).
[37]See supplementary material at http://dx.doi.org/10.1116/1.4766318 for detailed simulation data Tables S1–S9.
[38]S. Yasin, D. G. Hasko, and H. Ahmed, Appl. Phys. Lett. **78**, 2760 (2001).
[39]Y. Nakamura, T. Nakagawa, N. Sasaki, A. Yamagishi, and M. Nakata, Macromolecules **34**, 5984 (2001).
[40]Y. Nakamura, N. Sasaki, and M. Nakata, Macromolecules **35**, 1365 (2002).
[41]M. Nakata, Y. Nakamura, N. Sasaki, and Y. Maki, Phys. Rev. E **76**, 041805 (2007).
[42]M. Holz, S. R. Heil, and A. Sacco, Phys. Chem. Chem. Phys. **2**, 4740 (2000).
[43]S. M. Scheinhardt-Engels, F. A. M. Leermakers, and G. J. Fleer, Phys. Rev. E **68**, 011802 (2003).
[44]M. Stepanova, T. Fito, Z. Szabo, K. Alti, A. P. Adeyenuwo, K. Koshelev, M. Aktary, and S. K. Dew, J. Vac. Sci. Technol. B **28**, C6C48 (2010).